•Benchmark derivative-based pipelines with non-redundant feature selection against simpler baselines.
•Identify the most informative spectral regions for donor phenotyping.

IECM 2025 Conference
The 4th International Electronic Conference on Metabolomics
13–15 October 2025 | Online
MDPI

FTIR Spectroscopy of Allograft Perfusate Separates DCD and DBD Donors: Early Results

Luis Ramalhete* [1, 2, 3]; Rúben Araújo [2];Miguel Bigote Vierira [2, 3, 4]; Emanuel Vigia [2, 3, 5]; Ana Pena [5]; Sofia Carrelha [5]; Anibal Ferreira [2, 3, 4]; Cecilia RC Calado [6, 7]

[1] Blood and Transplantation Center of Lisbon, Instituto Português do Sangue e da Transplantação, Lisbon, Portugal; [2] NOVA Medical School, Faculdade de Ciências Médicas, Universidade NOVA de Lisboa, Lisbon, Portugal; [3] iNOVA4Health—Advancing Precision Medicine, Núcleo de Investigação em Doenças Renais, NOVA Medical School, Lisbon, Portugal; [4] Nephrology, Hospital Curry Cabral, Unidade Local de Saúde de São José; [5] Hepato-Biliary-Pancreatic and Transplantation Centre, Curry Cabral Hospital - Local Health Unit of S. José - Lisbon, Portugal; [6] ISEL—Instituto Superior de Engenharia de Lisboa, Instituto Politécnico de Lisboa; [7] Institute for Bioengineering and Biosciences (iBB), The Associate Laboratory Institute for Health and Bioeconomy-i4HB, Instituto Superior Técnico (IST), Universidade de Lisboa (UL)

INTRODUCTION & AIM

Kidney transplantation still faces a supply–demand gap, driving wider use of kidneys from donation after circulatory death (DCD). Compared with donation after brain death (DBD), DCD kidneys carry a higher risk of delayed graft function, even though medium-term outcomes can converge with good selection and preservation. This creates a practical need for rapid, objective, pre-implant phenotyping. Label-free FTIR spectroscopy of static cold-storage Celsior effluent offers a fast, consumable-free readout of biochemical injury signatures that could distinguish DCD from DBD at the point of care.

To test whether FTIR “fingerprints” of Celsior preservation-solution effluent can discriminate DCD from DBD kidneys using a simple, rapid workflow coupled to machine-learning analysis in a pilot, proof-of-concept study.

METHOD

• Samples: Celsior perfusate from kidney allografts (n=10; 5 DCD / 5 DBD, matched)
.• Acquisition: Mid-IR FTIR focusing on Amide I and fingerprint regions
.• Preprocessing: Standard QC and normalization; routine derivative processing.
• Modeling: Supervised classifiers; cross-validation; comparison of pipelines with derivative processing plus non-redundant feature selection versus simpler baselines.
• Outcome: Discrimination of donor type (DCD vs DBD).

RESULTS & DISCUSSION

Per donor characteristics were well balanced across groups with the expected higher terminal serum creatinine in DCD, while other demographics and comorbidities were comparable, supporting a fair comparison of spectral readouts, presented in Table 1,

Table 1. Summarizes the demographic and clinical characteristics of the two groups.

Feature	DBD	DCD	p-value
Age	54.0 [54.0–64.0]	53.0 [50.0–54.0]	0.397615 [1]
Sex (% female)	80%	80%	1 [2]
Weight	70.0 [65.0–70.0]	74.0 [74.0–80.0]	0.137564 [1]
Height	165.0 [160.0–165.0]	172.0 [165.0–175.0]	0.167938 [1]
Body mass index	25.7 [25.4–25.7]	25.0 [24.2–29.4]	0.834035 [1]
Hypertension (% yes)	60%	80%	1 [3]
Diabetes	80%	80%	1 [3]
Serum creatinine	0.6 [0.6–0.7]	1.1 [1.0–1.1]	0.045866 [1]
Urea	21.0 [14.0–27.0]	35.0 [22.0–36.0]	0.150794 [1]
Estimated Glomerular Filtration Rate	93.0 [90.0–103.0]	77.0 [60.0–79.0]	0.059327 [1]
Cardiorespiratory arrest (%yes)	40%	100%	0.166667 [3]

DBD Donation after Brain Death, DCD Donation after Circulatory Death, [1] Mann–Whitney U, [2] Chi-square, [3] Fisher’s exact; two-sided α=0.05.

Spectral quality was similar between DCD and DBD: Amide I SNR, spike-burden, and fingerprint cosine-similarity showed no significant differences, arguing against a technical bias driving separability and validating the dataset for downstream analyses. In unsupervised views built from second-derivative spectra, DCD and DBD tended to cluster apart in the fingerprint region using cosine-distance heat mapping with Ward clustering and multidimensional scaling, with no obvious outliers, an independent signal that complements the supervised results, presented in Table 2.

Table 2. Comparison of FTIR quality control metrics between DCD and DBD donor groups. Data are presented as median [IQR] and mean ± SD. Group differences were assessed with two-sided Mann–Whitney U tests. Rank-biserial correlation (r) is reported as an effect size.

Variable	DCD_median[IQR]	DBD_median[IQR]	DCD_mean±SD	DBD_mean±SD	U	p value	Rank-biserial_r
SNR_Amidel	77.16 [67.70, 80.41]	67.11 [20.74, 81.15]	97.64 ± 60.49	51.69 ± 36.80	16	0.5476	-0.28
Spike_count	12.00 [6.00, 53.00]	12.00 [8.00, 34.00]	26.40 ± 26.31	19.20 ± 14.60	13	1	-0.04
Cosine_fp	0.99 [0.99, 1.00]	0.99 [0.95, 1.00]	0.97 ± 0.06	0.98 ± 0.03	15	0.6905	-0.2

DBD Donation after Brain Death, DCD Donation after Circulatory Death.

Mean second-derivative spectra also diverged visibly in the ~1200–1415 cm⁻¹ band cluster and more moderately near ~1673 cm⁻¹, consistent with the features later selected by the classifier presented in figure 1.

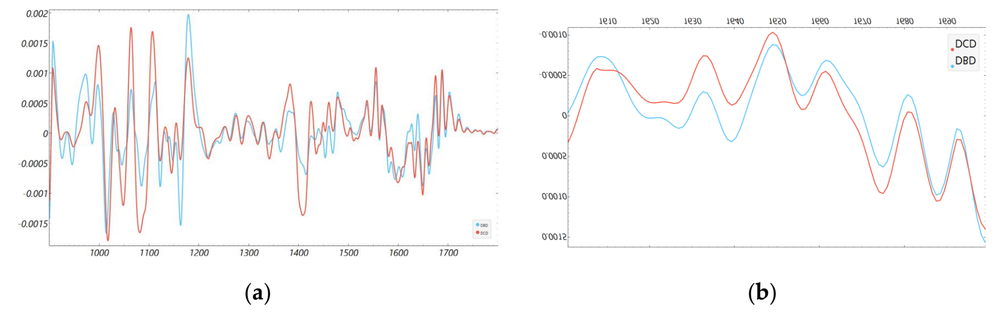

(a) (b)

Figure 1. 2nd derivative average FTIR spectra of donor groups. Mean spectra for DCD and DBD perfusion fluids in the fingerprint (900–1800 cm⁻¹) and Amide I (1600–1700 cm⁻¹) regions.

Supervised classification confirmed that the fingerprint window carried the most informative chemistry. With second derivative plus FCBF feature selection, SVM reached AUC 0.84 and 0.90/0.90/0.90 accuracy/sensitivity/specificity, while Naïve Bayes achieved AUC 1.00 with 1.00/1.00/1.00 accuracy/sensitivity/specificity under leave-one-out cross-validation, driven by wavenumbers around ~1202, ~1230, ~1342, and ~1413 cm⁻¹. In Amide I, discrimination improved only after derivative sharpening and feature filtering (peak ~1673 cm⁻¹), reaching AUC up to 0.92 but with more modest accuracy, underscoring that protein-backbone–dominated signal alone is less discriminative at this scale, presented in Table 3. Synchronous 2D-correlation maps further showed coordinated multi-band changes in the fingerprint and more moderate organization in Amide I, supporting that separation arises from structured co-variation rather than a single peak effect, presented in figure2.

Table 3. FTIR classification performance (LOOCV) for DCD vs DBD across spectral regions, preprocessing pipelines, and classifiers.

Model	Region	Preprocessing	AUC	Accuracy	Sensitivity	Specificity
SVM	Amide I 1600–1700 cm⁻¹	Rubber band BC	0.28	0.50	0.50	0.50
		VN	0.20	0.50	0.50	0.50
		1st derivative	0.32	0.30	0.30	0.30
		1st derivative + VN	0.24	0.70	0.41	0.70
		2nd derivative	0.60	0.80	0.60	0.80
		2nd derivative+ FCBF (~1673 cm-1)	0.88	0.90	0.70	0.70
Naïve Bayes		Rubber band BC	0.70	0.50	0.50	0.50
		VN	0.56	0.70	0.70	0.70
		1st derivative	0.48	0.50	0.50	0.50
		1st derivative + VN	0.62	0.70	0.70	0.70
		2nd derivative	0.80	0.80	0.60	0.90
		2nd derivative+ FCBF (~1673 cm-1)	0.92	0.70	0.70	0.70
SVM	Fingerprint 900–1800 cm⁻¹	Rubber band BC	0.36	0.00	0.00	0.00
		VN	0.20	0.30	0.30	0.30
		1st derivative	0.00	0.70	0.70	0.70
		1st derivative + VN	0.08	0.40	0.40	0.40
		2nd derivative	0.64	0.70	0.70	0.70
		2nd derivative+ FCBF (~1202, ~1203, ~1342, ~1413 cm-1)	0.84	0.90	0.90	0.90
Naïve Bayes		Rubber band BC	0.56	0.50	0.50	0.50
		VN	0.76	0.80	0.80	0.80
		1st derivative	0.74	0.70	0.70	0.70
		1st derivative + VN	0.86	0.80	0.80	0.80
		2nd derivative	0.88	0.80	0.80	0.80
		2nd derivative+ FCBF (~1202, ~1203, ~1342, ~1413 cm-1)	1.00	1.00	1.00	1.00

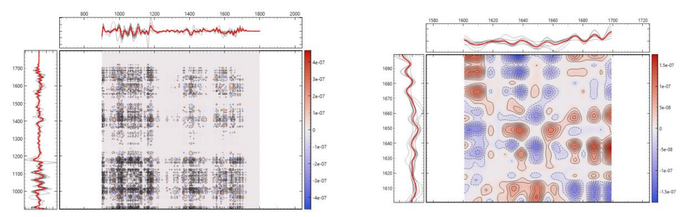

(a) (b)

Figure 2. Two-dimensional correlation spectroscopy (2D-COS) of 2nd derivative FTIR spectra. (a) Synchronous 2D correlation map of the fingerprint region (900–1800 cm⁻¹). (b) Synchronous 2D correlation map of the Amide I region (1600–1700 cm⁻¹). Cross-peaks highlight covarying vibrational bands, with intensity indicating the strength and direction of spectral correlations between donor groups.

CONCLUSION

- FTIR of Celsior effluent discriminates DCD vs DBD kidneys.
- Fingerprint region drives separation; key bands ~1202, 1230, 1342, 1413 cm⁻¹.
- Unsupervised clustering aligns with supervised results, not explained by QC differences.
- Best pipeline (2nd-derivative + FCBF, Naive Bayes) reached excellent LOOCV performance; SVM also strong.
- Amide I alone is less informative; derivative sharpening helps but remains secondary.
- Workflow is fast, label-free, and promising for point-of-care triage; larger validation is needed.

FUTURE WORK / REFERENCES

Prospectively validate in larger, multi-center cohorts with blinded pre-implant prediction and linkage to DGF, eGFR, and graft survival. Standardize the sampling/derivative workflow, stress-test models against confounders, and benchmark against perfusate biomarkers and pump metrics. Push toward bedside ATR-FTIR with automated QC, refine band attribution (~1202–1413/1673 cm⁻¹), perform external validation with locked models, and extend to other preservation solutions and donor profiles.